Detection of electric-quadrupole transitions in water vapour near 5.4 and 2.5 µm

Alain Campargue[a], Alexander M. Solodov[b], Alexander A. Solodov[c], Andrey Yachmenev[de], and Sergey N. Yurchenko[f]

Nowadays, the spectroscopic databases used for the modeling of the Earth and planetary atmospheres provide only electric-dipole transitions for polyatomic molecules (H_2O, CO_2, N_2O, CH_4, O_3…). Very recently, electric-quadrupole transitions have been detected in the high sensitivity cavity ring down spectrum (CRDS) of water vapour near 1.3 µm [A. Campargue et al. Phys. Rev. Res., 2 023091 (2020) DOI:10.1103/PhysRevResearch.2.023091]. This discovery paved the way to systematic searches of quadrupole transitions in water vapor and other polyatomic molecules. In the present work, on the basis of high accuracy *ab initio* predictions, $H_2{}^{16}O$ quadrupole lines are detected for the first time in the 5.4 µm and 2.5 µm regions where they are predicted to have their largest intensities (up to 10^{-26} cm/molecule). A total of twelve quadrupole lines are identified in two high sensitivity Fourier transform spectra recorded with a 1064 m path length. Ten lines in the 4030 - 4150 cm^{-1} region are assigned to the ν_3 band while the lines near 1820 and 1926 cm^{-1} belong to the ν_2 band. The derived line intensities which are largely above the dipole intensity cut-off of the standard spectroscopic databases, agree nicely with the theoretical predictions. We thus conclude that the calculated line list of quadrupole transitions, validated by the present measurements, should be incorporated in the spectroscopic databases.

[a] *Univ. Grenoble Alpes, CNRS, LIPhy, 38000 Grenoble, France E-mail: alain.campargue@univ-grenoble-alpes.fr*
[b] *Laboratory of Molecular Spectroscopy, V.E. Zuev Institute of Atmospheric Optics, Siberian Branch, Russian Academy of Sciences, 1, Academician Zuev sq.,634055, Tomsk, Russia*
[c] *Laboratory of Atmospheric Absorption Spectroscopy, V.E. Zuev Institute of Atmospheric Optics, Siberian Branch, Russian Academy of Sciences, 1, Academician Zuev sq., 634055, Tomsk, Russia*
[d] *Center for Free-Electron Laser Science, Deutsches Elektronen-Synchrotron DESY, Notkestraße 85, D-22607 Hamburg, Germany*
[e] *Center for Ultrafast Imaging, Universität Hamburg, Luruper Chaussee 149, 22761 Hamburg, Germany*
[f] *Department of Physics and Astronomy, University College London, London, WC1E 6BT, UK*

Introduction

In the infrared, molecular absorption spectra are in general due to electric-dipole (E1) rovibrational transitions. These transitions result from the coupling of the electromagnetic field with the transition electric-dipole moment induced by molecular vibrations. Spectroscopic databases such as HITRAN [1], GEISA [2] and ExoMol [3], provide extensive line lists of E1 transitions for the major atmospheric compounds (H_2O, CO_2, O_3, CH_4…), widely used for the analysis of telluric and planetary atmospheres. The electric-dipole moment of a homonuclear diatomic molecule (*e.g.* H_2, N_2, O_2) is null and these molecules do not show E1 absorption spectra. Nevertheless, these diatomic species may show extremely weak absorption lines due to a change in their electric-quadrupole (E2) moment. The E2 absorption lines are typically 10^6 times weaker than E1 lines which makes their detection extremely challenging. The first detection of E2 lines in a molecular spectrum was reported by Herzberg in 1949, using a 10 atm pressure of hydrogen and an absorption pathlength of 5.5 km [4]. Since then, E2 lines of H_2, O_2 and N_2 have been detected and used for remote sensing of the Earth [5-8] and planetary atmospheres [9,10]. In the laboratory, high sensitivity laser absorption methods have allowed to detect and characterize accurately E2 lines in H_2 [11,12], D_2 [13,14] and N_2 [15,16]. These observations including transitions among the weakest ever measured [11,15] provided stringent validation tests for the E2 line parameters computed theoretically [14,17]. In particular, the H_2 and D_2 spectra are accurately predicted by *ab initio* calculations including nonadiabatic, relativistic, and quantum electrodynamics (QED) corrections (see Ref. [18] and references therein). In the above mentioned databases, E2 transitions are provided (with theoretical parameters) only for H_2, O_2 and N_2 molecules that are not engaged in the E1 transitions, and are thus absent for polar diatomic and polyatomic molecules. Let us mention the special case of the HD isotopologue of hydrogen which has a small dipole moment and is the only species for which both E1 and E2 transitions were measured (see review included in [19]).

While usual absorption line lists of polyatomic molecules include very weak E1 lines (generally computed), the absence of quadrupole transitions questioned their completeness. In a recent work, some of us reported the first detection of electric-quadrupole transitions in water vapor by very high sensitivity cavity ring down spectroscopy (CRDS) near 1.3 µm [20]. The detection of E2 lines with intensity largely above the dipole transitions intensity cut-off (*e.g.* 10^{-29} cm/molecule for water in the HITRAN database) paved the way to systematic searches of E2 lines not only for water but also for major species such as CO_2, N_2O, HCN and polar diatomics like CO and HF. In Ref. [20], the detection of water E2 lines relied on high accuracy calculations of the $H_2{}^{16}O$ E2 spectrum. **Fig. 1** shows the superposition of the E2 and E1 calculated line lists of $H_2{}^{16}O$ with intensity in logarithmic scale. This figure illustrates the difficulty in detecting E2 lines in water because E2 bands are predicted to be very weak (less than 10^{-26} cm/molecule) and generally in coincidence with E1 bands which are stronger by a factor of 10^6 or 10^7. It is worth mentioning that differences in selection rules makes E2 and E1 transition frequencies distinct in $H_2{}^{16}O$ and thus E2 lines should in principle be observable. Nevertheless, they are generally hidden in

the line profile of the very dense and much stronger E1 lines. According to **Fig. 1**, the most favorable intervals for E2 detection are on the high energy side of the strong bands because *(i)* at low energy side is highly congested by hot band transitions; *(ii)* E2 lines following the $\Delta J = 2$ selection rule (*S* branch) extend to higher energy than the *R* branches ($\Delta J = 1$) of E1 bands. The region near 4100 cm^{-1} corresponding to the strongest predicted E2 transitions seems particularly favorable, even more favorable than the 7500 cm^{-1} region. In the present work, we report the first detection of E2 transitions near 4100 cm^{-1}: ten E2 lines were identified between 4030 and 4150 cm^{-1} in a long path absorption spectrum of natural water recorded in Tomsk by Fourier transform (FTS) spectroscopy. Additional FTS spectra were recorded in order to detect E2 lines in the 5 µm range. Although the strongest E2 lines have similar intensities than in the 2.5 µm region (about 10^{-26} cm/molecule), the E1 interfering lines are about ten times stronger which lowers the chances to detect an E2 line between E1 lines. Only two reliable E2 lines could be detected in that region.

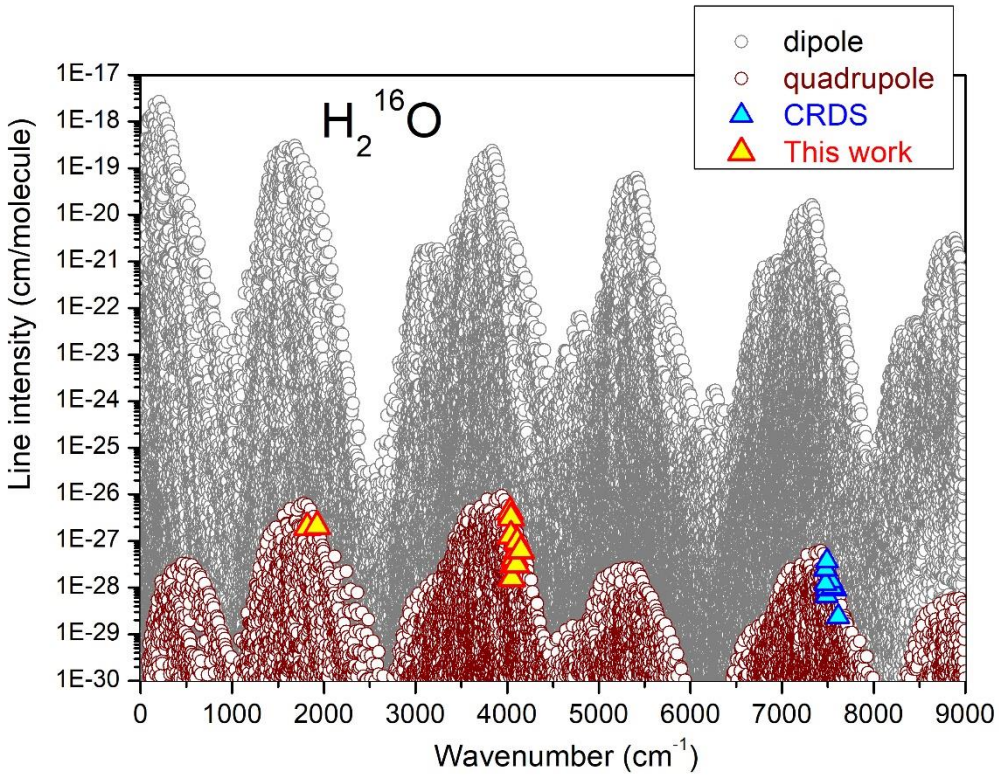

Fig. 1
Overview of the absorption line list of $H_2{}^{16}O$ at 296 K. The calculated electric-quadrupole spectrum [20] (wine circles) is superimposed to the calculated electric-dipole spectrum (grey circles). The red and blue triangles highlight the quadrupole transitions experimentally measured in this work by FTS and in Ref. [20] by CRDS, respectively.

Experiment

The absorption spectrum of water vapor was recorded using a high resolution Fourier transform infrared spectrometer (Bruker IFS 125 HR) coupled to a 30 meters multipass cell. The reader is referred to Ref. [21] for a detailed description of the set-up. The cell is equipped with a White-type three mirror

optical system. The diameter of the two back mirrors is 300 mm while the input front mirror is 500 mm×300 mm in size. The reflection coefficient of the mirrors for the visible and infrared regions exceeds 0.98. A long focal length mirror reduces the divergence of the light beam outgoing from the FTIR to diameters of 200 and 50 mm in the planes of back and front mirrors, respectively. This allowed us to minimize the losses of light inside the cell and increase the number of passes. The body of the spectrometer was evacuated to a residual pressure of ~ 0.025 mbar by means of a fore-vacuum pump, which helps to significantly reduce the absorption of atmospheric gases surrounding the cell.

Table 1. Thermodynamic and technical conditions of the recordings

Frequency range, (cm^{-1})	Radiation source	Detector	Resolution, (cm^{-1})	Number of acquisitions	Pathlength (m)	*T* (°C)	Pressure (mbar)
1800–2100	globar	LN2 cooled MCT	0.008	8220	1057.9	28.5	11.19
4000–5000	halogen lamp	LN2 cooled InSb	0.012	2000	1065.5	12.5	12.36

The absorption spectrum of natural water vapor was recorded in the 4000–5000 cm^{-1} region at a spectral resolution of 0.012 cm^{-1}. By using a 50 W halogen lamp as light source and a 1.5 mm diameter diaphragm, an optical path length of 1065.5 m corresponding to 38 passes could be achieved. The cell temperature during the recordings was 12.5 °C. The water vapor pressure, measured with a Baratron gauge with an estimated uncertainty of 0.25%, was fixed to 12.36 mbar. The transmitted light intensity was measured by a liquid nitrogen cooled InSb detector. In order to decrease the noise level, a spectral band-pass filter (maximum transmission of 80% at 2.2 µm, FWHM= 0.5 µm) was used and two thousand interferograms were co-added (total recording time of 16.6 hours). The noise level of the spectra, expressed as the RMS noise amplitude of the transmittance, was determined using the standard procedure of the OPUS 6.5 software. An average value of 10^{-4} was achieved. Taking into account the path length of 1065.5 m, it leads to a noise equivalent absorption coefficient, $\alpha_{min} \approx 10^{-9}$ cm^{-1} which corresponds to a detectivity threshold of about 5×10^{-28} cm/molecule for the water line intensities.

The experimental conditions of the recordings in the two investigated regions are summarized in **Table 1**. In the 1800–2100 cm^{-1} region, a globar was used as light source and the transmitted light intensity was measured with a liquid nitrogen cooled MCT detector. The values of the pressure and pathlength are similar to those of the 2.5 µm region. The cell temperature during the recordings was higher (28.5 °C). A total of 8220 interferograms were co-added, leading to a noise equivalent absorption coefficient ($\alpha_{min} \approx 5\times10^{-9}$ cm^{-1}) and a detectivity threshold (2×10^{-27} cm/molecule) about twice higher than in the 2.5 µm region.

Analysis

The identification of the E2 lines in the FTS spectrum was performed based on the agreement between the measured and calculated values for both line positions and line intensities. The quadrupole

spectrum of water was computed using the following well-established methodology based on a variational approach. We first solved the rovibrational Schrödinger equation for the motion of nuclei using the variational program TROVE [22,23] and a recently reported accurate potential energy surface of H_2O [24]. We have recently extended the TROVE package to treat triatomic molecules with access to the linear geometry [24], based on an exact kinetic energy operator form developed more than 30 years ago [25,26]. The rovibrational eigenfunctions generated together with energy levels were then employed to compute matrix elements of the quadrupole moment surface of H_2O using the RichMol program [27,28], designed for calculations of molecular ro-vibrational dynamics in the presence of external electro-magnetic fields. In these calculations a new *ab initio* quadrupole moment surface of H_2O was employed, generated with the CCSD(T)/aug-cc-pwCVQZ level of theory using the CFOUR program package [29].

In order to bring the quality of the line positions to the experimental accuracy, the variational energy levels of $H_2{}^{16}O$ were replaced by the corresponding empirical values from [30]. In this replacement we took advantage of the two-file structure of the ExoMol line list consisting of a states file and a transition file [3,31]. The resulting typical accuracy of 10^{-3} cm^{-1} in the line centers provides a crucial criterion for unambiguous identification of E2 lines.

Results

As illustrated on **Figs. 2 and 3**, the superposition of the calculated E2 line list to the recorded spectra leaves no doubt that E2 lines of $H_2{}^{16}O$ are detected in the two regions. All the E2 lines predicted with an intensity above the experimental detectivity threshold were systematically searched in the two FTS spectra. As a result, two and ten E2 lines were detected in the 5.4 μm and 2.5 μm regions, respectively.

It is important to underline that all the sufficiently strong predicted E2 lines were found either obscured by other lines or detected. Examples of E2 lines hidden by other absorption features are presented in **Fig. 4**. Note that E2 lines are hidden not only by E1 lines of the main isotopologue, $H_2{}^{16}O$, but also those of the minor isotopologues present in standard isotopic abundance (for instance 2×10^{-3} for $H_2{}^{18}O$). In addition, E2 lines may be obscured by lines of some impurities (CO_2, NH_3, OCS…) present at very low concentration in the used water sample. For instance, an NO doublet is observed near the E2 line near 1926.040 cm^{-1} (**Fig. 2**, lower panel) and OCS lines of the $2\nu_3$ band centered near 4100 cm^{-1} are identified (see lower panel of **Fig. 4**). The intensities of the detected NO and OCS lines are about 10^7 and 10^6 times stronger than those predicted for the nearby E2 lines. The NO and OCS relative abundances in the sample are calculated to be no more than a few ppm for both species.

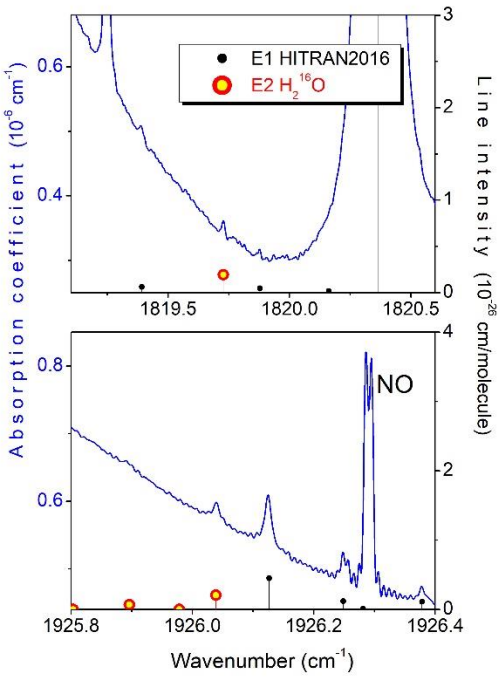

Fig. 2

Detection of electric-quadrupole lines of $H_2{}^{16}O$ in the spectrum of water vapour recorded by FTS at 11.19 mbar Torr in the 5.4 µm region. The calculated quadrupole spectrum of $H_2{}^{16}O$ (red stars) [20] is superimposed to the HITRAN (dipole) stick spectrum of water in natural isotopic abundance (black points) [1]. Note that the (common) intensity scale of the E1 and E2 stick spectra has been chosen to have the height of the E1 sticks roughly equal to the height of the corresponding E1 lines. The two detected quadrupole lines correspond to ΔJ= 2 transitions of the ν_2 band. A doublet due to NO present as an impurity with 6 ppm relative concentration is observed on the lower panel.

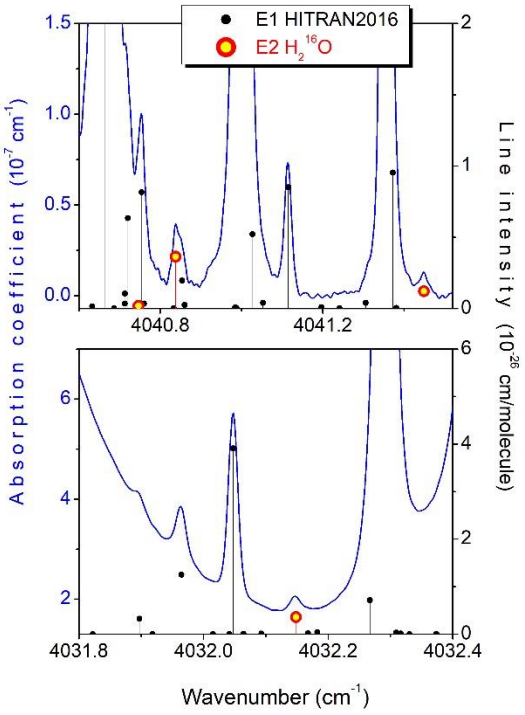

Fig. 3

Detection of electric-quadrupole lines of $H_2{}^{16}O$ in the 2.5 µm range. The calculated quadrupole spectrum of $H_2{}^{16}O$ (red circles) [20] is superimposed to the HITRAN (dipole) stick spectrum of water in natural isotopic abundance (black points) [1]. The three detected quadrupole lines are ΔJ= 2 transitions of the ν_3 band.

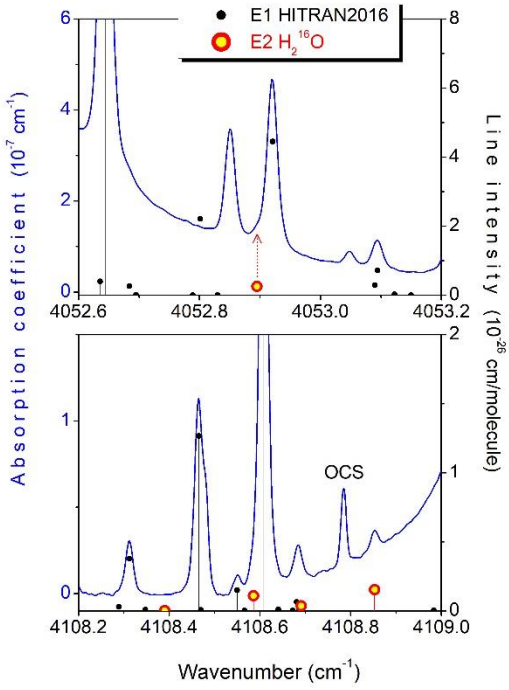

Fig. 4

Examples of predicted electric-quadrupole lines of $H_2{}^{16}O$ (red circles) hidden by other absorption features. Only the E2 line at 4108.852 cm^{-1} (lower panel) can be reliably measured. Note the inaccurate HITRAN position for the line at 4052.848 cm^{-1} due to $H_2{}^{17}O$ (upper panel) and the line near 4108.785 cm^{-1} due to OCS present as an impurity with a ppm relative concentration (lower panel).

The experimental positions and intensities of the E2 lines were retrieved by using a homemade interactive least squares multi-lines fitting written in LabVIEW with a Voigt profile for the line shape. The comparison of the derived values to the theoretical results shows an overall good agreement (**Table 2).** Experimental intensity values range between 2×10^{-28} and 4×10^{-27} cm/molecule. Obviously the weakness and blending of E2 lines lead to large uncertainties in the reported intensities. In the most favorable cases corresponding to the three lines displayed on **Fig. 3**, the intensity agreement is better than 20 %.

As for the line positions, the present measurements with an estimated uncertainty of 2×10^{-3} cm^{-1} are not expected to improve the knowledge of the energy levels involved in the observed E2 transitions. The agreement with the predicted values within 10^{-3} cm^{-1} for most of the lines is thus fully satisfactory.

The rovibrational assignments included in **Table 2** indicate that all lines correspond to ΔJ= 2 transitions. The two lines in the 5.4 µm region belong to the ν_2 bending band while in the 2.5 µm region, one transitions belong to the ν_1 symmetric stretching band and others.to the antisymmetric stretching band, ν_3.

Table 2

Assignment, transition frequencies, and intensities of the electric-quadrupole lines of $H_2{}^{16}O$ measured near 5.4 and 2.5 µm and comparison with theoretical values [20].

Position (cm^{-1})		Int. (cm/molecule) [b]		Band	$J\ K_a\ K_c$					
Meas.	Emp. [a]	Meas.	Calc.		Upper level			Lower level		
1819.727	1819.728	1.12E-27	1.98E-27	ν_2	6	0	6	4	0	4
1926.040	1926.039	1.64E-27	1.93E-27	ν_2	9	0	9	7	0	7
4032.147	4032.148	4.22E-27	3.65E-27	ν_3	5	3	3	3	2	1
4040.838	4040.838	3.13 E-27	3.50 E-27	ν_3	8	0	8	6	1	6

4041.450	4041.449	1.29 E-27	1.17 E-27	ν_3	8	1	8	6	0	6
4052.893	4052.895	1.56 E-28	2.51 E-28	ν_3	7	2	6	5	1	4
4071.454	4071.455	3.11 E-28	8.36 E-28	ν_3	6	3	4	4	2	2
4083.035	4083.031	4.24 E-28	4.82 E-28	ν_3	8	2	7	6	1	5
4100.719	4100.718	3.11 E-28	2.69 E-28	ν_1	7	2	5	5	0	5
4106.763	4106.763	6.17 E-28	1.49 E-27	ν_3	7	3	5	5	2	3
4108.852	4108.853	9.51 E-28	1.51 E-27	ν_3	6	4	2	4	3	2
4150.162	4150.163	6.25 E-28	9.56 E-28	ν_3	7	4	4	5	3	2

Note

[a] Line positions computed according to empirical energy values of the lower and upper energy levels [30]

[b] The measured and calculated [20] intensity values are given at the temperature of the spectra recordings: 301.7 and 285.7 K in the 5.4 and 2.5 µm range, respectively.

Conclusion

Up to recently, it was considered to be unlikely that electric-quadrupole transitions would be observed in spectra of polyatomic molecules at room-temperature. Being 10^6-10^7 times weaker, E2 lines were believed to be totally obscured by electric-dipole transitions. On the basis of theoretical predictions obtained from newly developed high accuracy variational approach, the first detection of E2 lines in a polyatomic molecule was reported for water vapor by using highly-sensitivity cavity ring down spectroscopy near 1.3 µm [20]. In the present work, state-of-the-art Fourier transform spectroscopy allowed for new detections in water vapor spectra in the 2.5 and 5.4 µm regions. By coupling an FT spectrometer to a 30 meters multipass cell, a kilometric path length was achieved providing a noise equivalent absorption coefficient at the $\alpha_{min} \approx 10^{-9}$ cm^{-1} level. In addition to the required sensitivity, the detection of E2 lines was only possible in some narrow spectral intervals mostly free of the contribution from the much stronger dipole transitions. In that context, the large spectral coverage provided by the FTS technique was a crucial advantage.

Of first importance for the search of E2 lines in water vapour is the quality of the theoretical intensities which are now validated in three spectral regions. The calculated E2 list provide positions adjusted according to empirical energy levels [30] with a typical accuracy of 10^{-3} cm^{-1}, corresponding to a fraction of the Doppler width. The position agreement was used as critical criterion for the discrimination of E2 lines in the very dense spectrum resulting from the sensitivity of the recordings ($\alpha_{min} \approx 10^{-9}$ cm^{-1}). The experimental validation of the calculated line intensities is presently demonstrated not only by the agreement with the measured values within the experimental error bar, but also by the fact that, in absence of interference with E1 lines, all the predicted E2 lines with intensity above the experimental sensitivity threshold were detected.

A large number of quadrupole lines have intensities largely above the standard dipole intensity cut-off of spectroscopic databases and should thus be incorporated (see **Fig. 1**). For instance, the strongest E2 lines near 4000 cm^{-1} have an intensity three orders of magnitude higher than the HITRAN intensity cut-off at 10^{-29} cm/molecule.

As a result of their weakness, the E2 lines will have marginal impact on the radiative budget of the Earth atmosphere. Nevertheless, they may impact a number of atmospheric applications based on the monitoring of specific water absorption lines. This is the case in geosciences where very small variation of abundance ratios of water minor isotopologues are measured to trace various chemical and physical processes (see *e.g.* Refs. [32-34]). Any accidental coincidence between an E2 line of the main isotopologue and the monitored (weak) absorption lines of the water minor isotopologues will skew the retrieved isotopic abundances.

The present results indicate that E2 transitions have to be systematically computed for all standard atmospheric polar diatomic and polyatomic molecules, in particular CO_2 and CO. In the case of water vapour, the E1 and E2 bands mostly coincide but, for different molecular symmetry and corresponding selection rules, E2 bands may be located in regions of weak E1 absorption (transparency windows) and thus have a much higher relative importance.

ACKNOWLEDGMENTS

SY acknowledges support from the UK Science and Technology Research Council (STFC) No. ST/R000476/1. A substantial part of the calculations was performed using high performance computing facilities provided by DiRAC for particle physics, astrophysics and cosmology and supported by BIS National E-infrastructure capital ~~grant ST/J005673/1 and STFC grants ST/H008586/1, ST/K00333X/1~~. The work of A.Y. has been supported by the Deutsche Forschungsgemeinschaft (DFG) through the clusters of excellence "Center for Ultrafast Imaging" (CUI, EXC 1074, ID 194651731) and "Advanced Imaging of Matter" (AIM, EXC 2056, ID 390715994).

References

1. I.E. Gordon, L.S. Rothman, C. Hill, R.V. Kochanov, Y. Tan, P.F. Bernath, M. Birk, V. Boudon, A. Campargue, K.V. Chance, B.J. Drouin, J.-M. Flaud, R.R. Gamache, J.T. Hodges, D. Jacquemart, V.I. Perevalov, A. Perrin, K.P. Shine, M.-A.H. Smith, J. Tennyson, G.C. Toon, H. Tran, V.G. Tyuterev, A. Barbe, A.G. Császár, V.M. Devi, T. Furtenbacher, J.J. Harrison, J.-M. Hartmann, A. Jolly, T.J. Johnson, T. Karman, I. Kleiner, A.A. Kyuberis, J. Loos, O.M. Lyulin, S.T. Massie, S.N. Mikhailenko, N. Moazzen-Ahmadi, H.S.P. Müller, O.V. Naumenko, A.V. Nikitin, O.L. Polyansky, M. Rey, M. Rotger, S.W. Sharpe, K. Sung, E. Starikova, S.A. Tashkun, J. Vander Auwera, G. Wagner, J. Wilzewski, P. Wcislo, S. Yu and E.J. Zak, *J. Quant. Spectrosc. Radiat. Transfer,* 2017, 203, 3–69.
2. N. Jacquinet-Husson, R. Armante, N. A. Scott, A. Chedin, L. Crepeau, C. Boutammine, A. Bouhdaoui, C. Crevoisier, V. Capelle, C. Boonne, N. Poulet-Crovisier, A. Barbe, D. Chris Benner, V. Boudon, L. R. Brown, J. Buldyreva, A. Campargue, L. H. Coudert, V. M. Devi, M. J. Down, B. J. Drouin, A. Fayt, C. Fittschen, J. M. Flaud, R. R. Gamache, J. J. Harrison, C. Hill, O Hodnebrog, S. M. Hu, D. Jacquemart, A. Jolly, E. Jiménez, N. N. Lavrentieva, A. W. Liu, L. Lodi, O. M. Lyulin, S. T. Massie, S. Mikhailenko, H. S. P. Muller, O. V. Naumenko, A. Nikitin, C. J. Nielsen, J. Orphal, V. I. Perevalov, A. Perrin, E. Polovtseva, A. Predoi-Cross, M. Rotger, A. A. Ruth, S. S. Yu, K. Sung, S. A. Tashkun, J. Tennyson, Vl G. Tyuterev, J. Vander Auwera, B. A. Voronin, and A. Makie, *J. Mol. Spectrosc.,* 2016, 327, 31–72.
3. J J. Tennyson, S.N. Yurchenko, A.F. Al-Refaie, E.J. Barton, K.L. Chubb, P.A. Coles, S. Diamantopoulou, M.N. Gorman, C. Hill, A.Z. Lam, L. Lodi, L.K. McKemmish, Y. Na, A. Owens, O.L. Polyansky, T. Rivlin, C. Sousa-Silva, D.S. Underwood, A. Yachmenev and E. Zak, J. Mol. Spectrosc., 2016, 327, 73–94.
4. G. Herzberg, *Nature,* 1949, 163, 170–170.
5. L. S. Rothman and A. Goldman, *Applied Optics*, 1981, 20, 2182–2184.
6. A. Goldman, J. Reid and L. S. Rothman, *Geophys. Res. Lett.*, 1981, 8, 77–78.
7. C. Camy-Peyret, J.-M. Flaud, L. Delbouille, G. Roland G, J. W. Brault and L. Testerman, *J. Phys. Lett.*, 1981, 42, L279–L283.
8. P. Rinsland, R. Zander, A. Goldman, F. J. Murcray, D. G. Murcray, M. R. Gunson and C. B. Farmer, *J. Mol. Spectrosc.,* 1991, 148, 274–279.
9. K. H. Baines, M. E. Mickelson, L. E. Larson and D. W. Ferguson, *Icarus*, 1995, 114, 328–340.
10. W. H. Smith and K. H. Baines, *Icarus*, 1990, 85, 109–119.
11. A. Campargue, S. Kassi, K Pachucki and J. Komasa, *Phys. Chem. Chem. Phys.*, 2012,14, 802–815.
12. S. -M. Hu, H. Pan, C.-F Cheng, X.-F. Li, J. Wang, A. Campargue and A.W. Liu, A*strophys. J.*, 2012, 749, 76.
13. S. Kassi, A. Campargue, K. Pachucki and J. Komasa, *J. Chem. Phys.*, 2012, 136, 184309.
14. P. Wcisło, F. Thibault, M. Zaborowski, S. Wójtewicz, A. Cygan, G. Kowzan G, et al., *J. Quant. Spectrosc. Radiat. Transfer,* 2018, 213, 41–51.
15. S. Kassi. and A. Campargue, *J. Chem. Phys.*, 2012, 137, 234201.
16. P. Čermák, S. Vasilchenko, D. Mondelain, S. Kassi and A. Campargue, *Chem. Phys. Lett.*, 2017, 668, 90–94.
17. H. Li and R. J. Le Roy, *J. Chem. Phys.*, 2007, 126, 224301.
18. K. Pachucki and J. Komasa, *Phys. Chem. Chem. Phys.*, 2019, 21, 10272–10276.
19. S. Vasilchenko, D. Mondelain, S. Kassi, P. Čermák, B. Chomet, A. Garnache, S. Denet, V. Lecocq and A. Campargue, *J. Mol. Spectrosc.*, 2016, 326, 9–16.
20. A. Campargue, S. Kassi, A. Yachmenev, A.A. Kyuberis, J. Küpper and S. N. Yurchenko, *Phys. Rev. Res.*, 2020, 2, 023091.
21. Y. N. Ponomarev, A. A. Solodov, A. M. Solodov, T. M. Petrova and O. V. Naumenko, *J. Quant. Spectrosc. Radiat. Transfer,* 2016, 177, 253–260.
22. S. N. Yurchenko, A. Yachmenev, and R. I. Ovsyannikov, *J. Chem. Theory Comput.*, 2017, 13, 4368–4381.
23. O. L. Polyansky, N. F. Zobov, I. I. Mizus, L. Lodi, S. N. Yurchenko, J. Tennyson, A. G. Császár, and O. V. Boyarkin, *Phil. Trans. Royal Soc. London A*, 2012, 370, 2728–2748.
24. S. N. Yurchenko and T. Mellor., *in preparation*, (2020).
25. S. Carter S., N. C. Handy, and B.T. Sutcliff, *Mol. Phys.*, 1983, 49, 745–748.
26. B. T. Sutcliffe and J. Tennyson. *Intern. J. Quantum. Chem.*, 1991, 39, 183–196.
27. A. Owens and A. Yachmenev. *J. Chem. Phys.*, 2018, 148, 124102.
28. A. Yachmenev, L. V. Thesing, and J. Küpper, Laser-induced dynamics of molecules with strong nuclear quadrupole coupling, *J. Chem. Phys.*, 2019, 151, 244118.
29. CFOUR, Coupled-Cluster techniques for Computational Chemistry, a quantum chemical program package written by Stanton J. F. et al. and the integral packages MOLECULE (J. Almlöf. and P.R. Taylor), PROPS (P. R. Taylor.), ABACUS (T. Helgaker et al.), and ECP routines by A. V. Mitin and C. van Wüllen. For the current version, see http://www.cfour.de (2018).

30. J. Tennyson, P. F. Bernath, L. R. Brown, A. Campargue, M. R. Carleer, A. G. Császár, et al., *J. Quant. Spectrosc. Radiat. Transfer*, 2009, 110, 573–596.
31. J. Tennyson and S. N. Yurchenko. *Mon. Not. R. Astron. Soc.*, 2012, 425, 21–33.
32. E. R.Th. Kerstel and H.A.J. Meijer, Optical Isotope Ratio Measurements in Hydrology (Chapter 9), in: Isotopes in the Water Cycle: past, present and future of a developing science. pp. 109-124, P.K. Aggarwal, J. Gat, and K. Froehlich (Eds.), IAEA Hydrology Section, Kluwer, 2005.
33. J. B. McManus, D. D. Nelson, and M. S. Zahniser, *Optics Express*, 2015, 23, 6569–6586.
34. E. J. Steig, V. Gkinis, A. J. Schauer, S. W. Schoenemann, K. Samek, J. Hoffnagle, K. J. Dennis, and S. M. Tan, *Atmospheric Measurement Techniques Discussions* 2013, **6,** 10191–10229.